Segmentation of the Biliary Tree in MRCP Data

Kevin Robinson[a], Paul F Whelan[a] and John Stack[b]

[a]Vision Systems Laboratory, Dublin City University, Ireland
[b]Division of Radiology, Mater Misericordiae Hospital, Dublin, Ireland

ABSTRACT

Magnetic Resonance Cholangiopancreatography (MRCP) is a type of MR imaging which utilises protocols designed to enhance stationary fluids in the imaged volume. In this way it visualises the pancreatobiliary tract by highlighting the bile and pancreatic juices in the system. Current practice sees this data being assessed directly, with little or no processing being performed prior to review. MRCP data presents three main difficulties when it comes to image processing. The first is the relatively noisy nature of the data. Second is its low spatial resolution, especially in the inter-slice direction. And third, the variability observed between MRCP studies, which makes consistent results difficult to attain. This paper describes the initial phase of research which aims to develop assistive image analysis techniques to aid in the interpretation of MRCP data. The first stage in this process is the robust segmentation of the pancreatobiliary system. To this end a segmentation procedure has been developed using an approach based on the tools and techniques of the mathematical morphology. This paper examines the task at hand and presents initial results, describing and assessing the segmentation approach developed.

Keywords: MRCP, Biliary Tree, Liver, Morphology, Segmentation

1. INTRODUCTION

Much work has been reported into the use of MRCP in the imaging and assessment of the pancreatobiliary tract. However most of the published research to date approaches the topic from the point of view of an MR imaging problem. Many investigations have been conducted developing and comparing various MRI protocols, and assessing the effectiveness and utility of raw MRCP as a diagnostic imaging technique,[1–4] however little work has been reported on the application of data post-processing techniques in order to enhance the presentation and interpretation of the data.

Some research has been conducted into the reconstruction of the biliary tree from orthogonal projections,[5,6] and work has been published demonstrating a simple virtual endoscopic approach to the review of MRCP data.[7] Much work has also been reported on in the similar problem areas of the segmentation and reconstruction of vascular trees, using data from various imaging modalities.[8–10] In general MRCP data exhibits poorer resolution and noise characteristics than that from the modalities used in these other applications. Hence the effective assessment and analysis of MRCP data represents an important challenge in the development of MRCP as a valuable diagnostic tool in its own right.

2. METHOD

The approach taken in this work involves the application of image processing techniques based on the mathematical morphology[11,12] to filter and segment the raw data prior to visualisation using a surface rendering approach. The main segmentation step is performed using a three dimensional implementation of the watershed algorithm.[13] The effectiveness of segmentation using this technique is strongly influenced by the characteristics of the gradient function used to generate the input to the algorithm. The selection of a gradient function for

Further author information: (Send correspondence to K.R.)
K.R: E-mail: kevin.robinson@eeng.dcu.ie, Web: http://www.eeng.dcu.ie/~vsl
P.F.W: E-mail: paul.whelan@eeng.dcu.ie, Web: http://www.eeng.dcu.ie/~whelanp/home.html
J.S.: E-mail: jstack@mater.ie, Web: http://www.mater.ie/depts/radiology

our purposes was most particularly guided by the requirement that the narrow and often faint branches of the biliary tree must be reliably isolated, and so the gradient function used must demonstrate good differentiation in these cases.

2.1. Gradient function

Many approaches exist for calculating gradient information in image and volume data, starting with the simplest forms of neighbourhood difference calculation, and taking in such filtering techniques as sobel and its variants.

For our purposes it is essential that the selected approach perform well when faced with gradients present over only a very small number of voxels. The smaller hepatic branches in particular may appear as only one or two voxels across in the data, as in Figure 1. When faced with a rising edge followed closely by a falling edge some operators even act to attenuate the gradient signal in these regions.

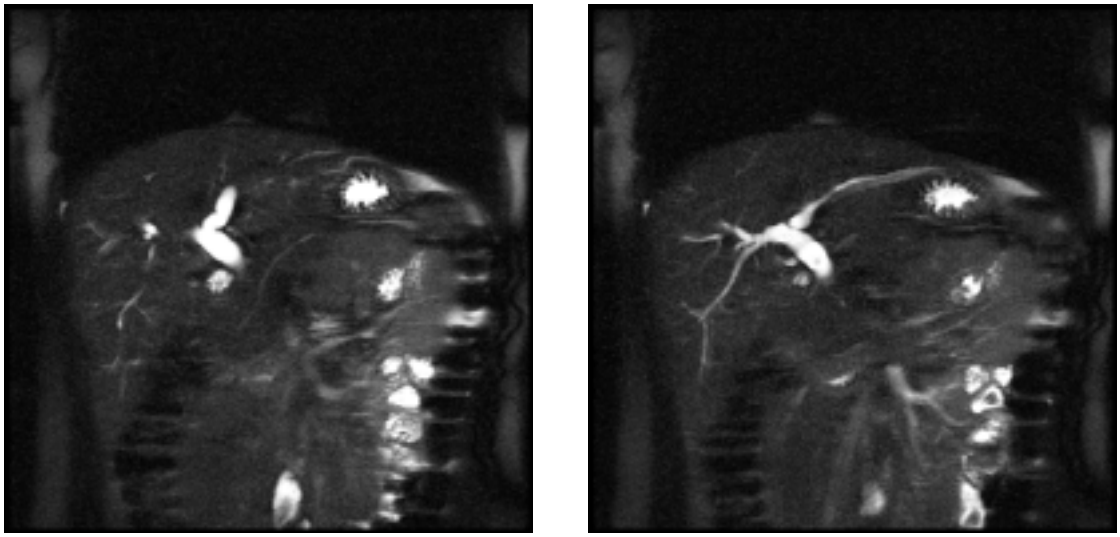

Figure 1. Raw MRCP Data.

A large number of operators were investigated and assessed, being applied in both their two dimensional and three dimensional forms. That is to say that gradients were calculated and segmentations performed both slice by slice and taking the volume as a whole. Each approach has its advantages and disadvantages but based on our requirements a three dimensional approach proved to be the best choice.

Within the class of three dimensional gradient functions investigated the one which exhibited the best characteristics for this application proved to be a three dimensional implementation of the morphological greyscale external gradient function. The standard morphological gradient function is calculated as the difference between the dilation of an image, and its erosion. The internal and external variants are defined respectively as the original data minus its erosion, and the dilation minus the original data.

The external gradient function has very desirable characteristics for our purposes. When using watershed segmentation it is of no utility if the smaller ducts result in long narrow peaks in the gradient image, no matter how intense. In order for the segmentation step to assign these branch voxels to the biliary tree object a lower intensity path must exist between the peaks representing the two edges of the ducts. This reflects the nature of the segmentation algorithm, which is a region growing rather than a boundary tracking process. The images in Figure 2 demonstrate well this characteristic of the morphological external gradient function. Note especially the small descending branch to the left of the images. The gradient images shown correspond to the two raw images in Figure 1. These are two adjacent slices mid way through a coronally acquired MRCP data set

consisting of 15 slices in total, each 256 × 256 pixels. The spacial resolution of the data is 1.17mm × 1.17mm × 4.0mm in the x, y, and z directions respectively.

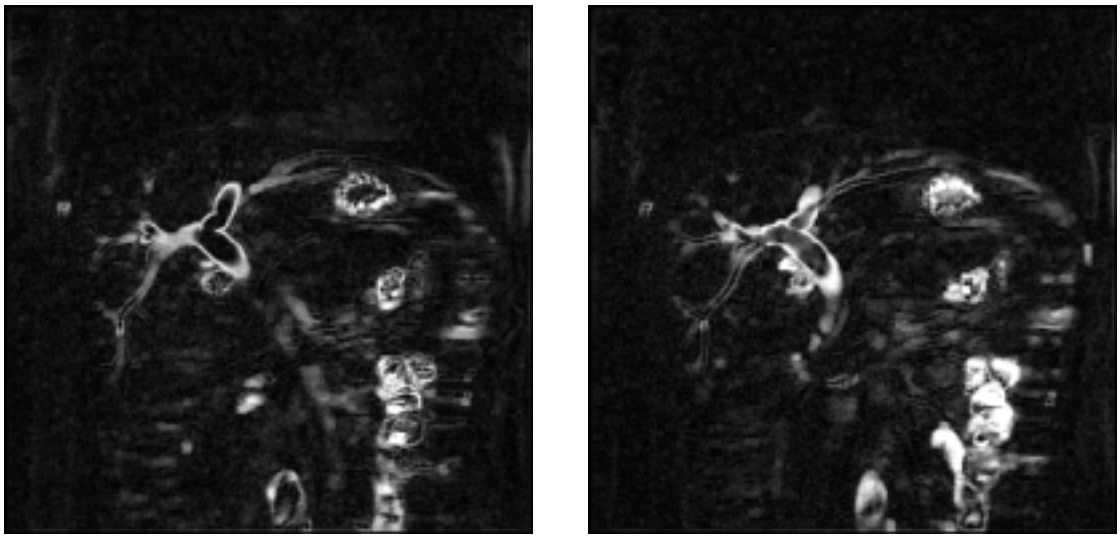

Figure 2. Output from the gradient function.

2.2. Label guided watershed segmentation

Once the gradient volume has been generated labels are added, derived from a simple thresholding of the original data. The bile along with gastrointestinal and other fluids appear as high intensity signal and so a threshold robustly provides seed regions for the label based watershed segmentation step which follows. After discarding small connected regions the main high intensity areas of the data, including the biliary tree are seeded ready for segmentation.

The watershed process itself proceeds by associating voxels with the labelled region which their expanding flood plane first meets. Flooding proceeds from low intensity to high intensity voxels, successively classifying the voxels at each level. When two labelled regions meet the set of voxels at their interface are classified as crest voxels. The three dimensional watershed algorithm guarantees that each region is completely isolated from all neighbouring regions by a closed, unit thickness, twenty-six connected surface of crest voxels.

Figure 3 continues the progression started in the previous two figures and shows the result of watersheding on the same two slices. The grey region has been classified as background, the black regions represent the various objects which have been isolated, each one has its own label, and the white represents the voxels classified as crest voxels. Unlike the two dimensional case crest voxels in a three dimensional watershed form a surface. Thus whole regions within a slice can be classified as crest, as can be seen in both of the images in Figure 3. This situation represents the case where the boundary is separating a region in the slice above from a region in the slice below.

2.3. Triangulated surface generation and display

Once segmentation is complete the labelled region corresponding to the biliary tree is processed in order to extract a triangulated surface representation of the tree. First a threshold level is calculated. This is achieved by examining each location where a transition between biliary and crest voxels is found. The range of grey levels separating these two voxels in the original data is recorded in each case. A threshold level is then selected which maximises the number of transitions which bracket the threshold. This approach guarantees that the smoothest possible surface will be fitted to the data.

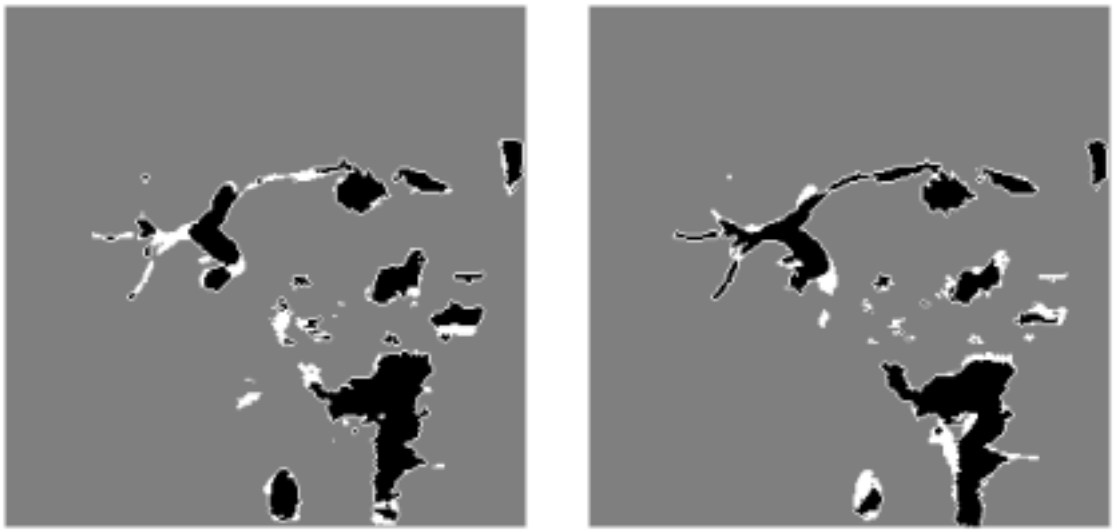

Figure 3. Results of the segmentation.

For transitions that bracket the selected threshold value the placement of the surface intersection is interpolated to an appropriate position along the line connecting the two voxels. The interpolation range is limited to exclude a small section at each end of the line. This is done to avoid the generation of degenerate triangles, i.e. triangles with two or three coincident vertices, which would thus reduce to lines and points respectively.

When the values of a transition pair both lie to one or other side of the threshold the surface intersection point is placed at the appropriate extreme of the interpolation range, i.e. towards the object if both voxel values lie below the threshold, and away from the object if both voxel values lie above the threshold. This rule reflects the fact that the bile is high intensity and the background tissue is low intensity.

The triangle mesh is generated using a scheme similar to the marching cubes approach,[14] with successive surface patches being calculated for each $2 \times 2 \times 2$ region in the volume. Once completed the triangulated surface is visualised using a standard Phong surface rendering algorithm[15] as illustrated in Figure 4. Animation and interactive fly through are possible, including overlay of the original voxel data, in order to examine and assess the data in a flexible and informative way.

3. RESULTS

The data set illustrated in the previous section represents the 'good' end of the MRCP spectrum: minimal motion and other artifacts, good contrast in the major ducts of the biliary tree, relatively clean and noise free data, minimal interference from extraneous signals (gastrointestinal fluid etc.), and good localisation of the liver within the imaged volume.

The database of fifty four MRCP studies used in the development and assessment of this segmentation process includes among its elements examples demonstrating the other end of this spectrum in all the aspects mentioned above. The variability observed within the database studies is due in part to the fact that the studies were conducted over a period of time during which ongoing experimentation and development of the MRI protocols being used was underway. However this is by no means the only source of variability. The time taken for image acquisition, and the resultant susceptibility to motion artifacts in particular remains a major difficulty. It is clear that the protocols currently available all produce results of considerable variability.

The problem of variability will always exist to some extent, as much of it can also be attributed to actual differences in the biliary trees being imaged. For instance a grossly dilated tree filled with bile unsurprisingly

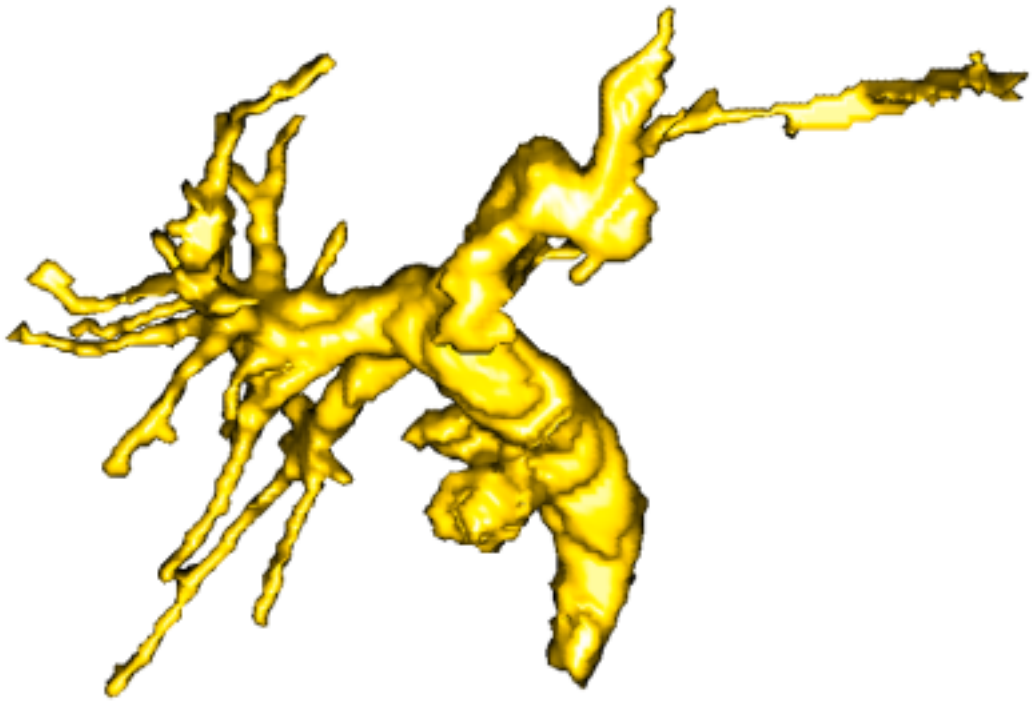

Figure 4. Surface rendering of segmented biliary tree.

results in a stronger signal in the data and a more clearly defined tree for segmentation. Thus it is not unexpected that, while some data sets can yield a segmentation of considerable detail, others may result in the segmentation of no more than a small section of the biliary tree. This is not to say that all is lost. As addressed in the next section, with reference to future work, the results obtained to date form a solid basis for the ongoing programme of research planned.

The results presented in Figures 5, 6 and 7 demonstrate a range of segmentations achieved with the current approach. The images on the left are maximum intensity projections of the data sets, and illustrate the degree to which the biliary tree was visible in the raw data. The images on the right are surface renderings of the segmented data demonstrating the level of segmentation achieved in each case.

Figures 5a and 5b show the data set used earlier to illustrate section 2. This is an example of a good segmentation. All the major sections of the biliary tree have been isolated, including many of the smaller branches of the hepatic ducts.

Figures 6a and 6b illustrate an instance where the biliary signal is faint, and to a great extent swamped by widespread gastrointestinal signal. The segmentation in Figure 6b shows the common bile duct up as far as the primary bifurcation at the left and right hepatic ducts. Attempting to adjust the parameters in order to capture more of the biliary tree results in signal from the neighbouring bowel region being attached to the segmented object. An example of this happening can be seen in Figures 6c and 6d, where the lower region of the rendered surface represents a section of bowel proximal to the common bile duct which has remained attached in the segmentation process.

Figures 7a to 7d demonstrate two more good segmentations on varying data sets. In the first the gall bladder is not evident at all in the data while in the second it shows up very large and distinct. In both cases the common bile duct, and left and right hepatic ducts are imaged in some detail.

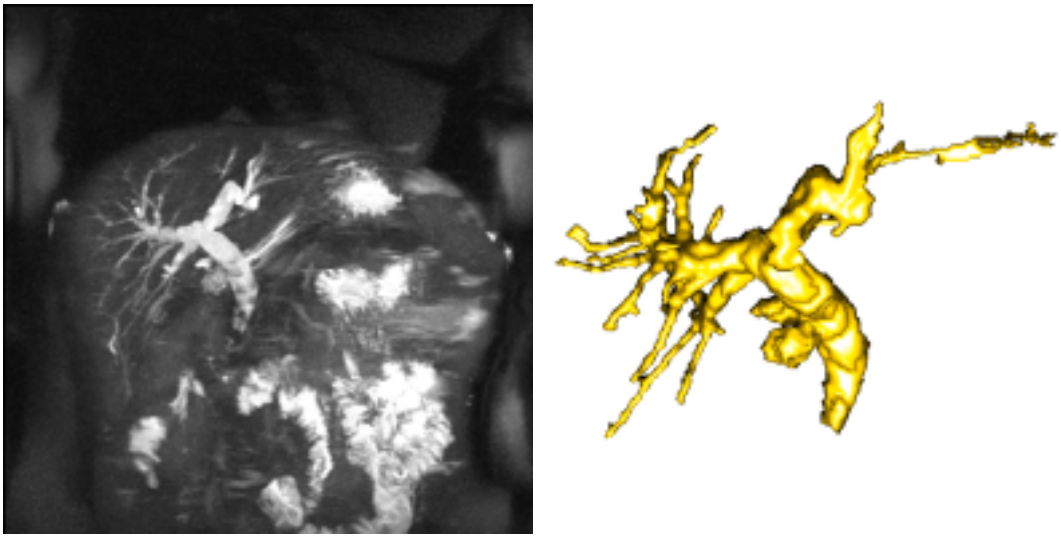

(a) (b)

Figure 5. Results obtained on various data sets.

As illustrated in these results the process of robustly isolating the biliary system in MRCP data is not a trivial one. However we have demonstrated that it is an achievable goal and one towards which this work takes a significant first step.

4. DISCUSSION AND FURTHER WORK

The segmentation process described here has been developed and tested using coronally acquired MRCP data sets demonstrating a range of pancreatobiliary tract pathologies. The process continues to be developed and improved but has so far demonstrated both the principles and the difficulties involved.

The figures included in this paper demonstrate on the whole a good level of segmentation in the smaller and fainter ducts present in the data. The particular challenges faced in processing data of the type available from MRCP examination present a difficult problem which when addressed will pave the way for the more widespread adoption of MRCP as the examination of choice in the assessment of the pancreatobiliary system.

The utilisation of effective image processing techniques combined with high quality surface and volume rendering will allow MRCP data to be reviewed and assessed in a versatile fashion integrating two and three dimensional views, and flexible navigation and interrogation tools, to form a unified review solution providing the best possible presentation of information and cues for interpretation to the radiologist.

With a good baseline segmentation established the next phase of the research will aim to improve the approach in a number of ways. Four main areas are identified, where this effort will be targeted.

- *Automation of manual steps*: selection of the threshold level for watershed label generation, and selection of the biliary tree object from the collection of segmented objects are currently achieved manually.
- *Improved segmentation*: robust segmentation of the smaller hepatic ducts will require the application of advanced image processing techniques.
- *Development of an interpretive model*: important in the development of assistive analysis tools is the interpretation of the data, identifying the main sections of the biliary tree (the gall bladder and the primary ducts), and detecting and highlighting the presence of features such as stones in the gall bladder and common bile duct.

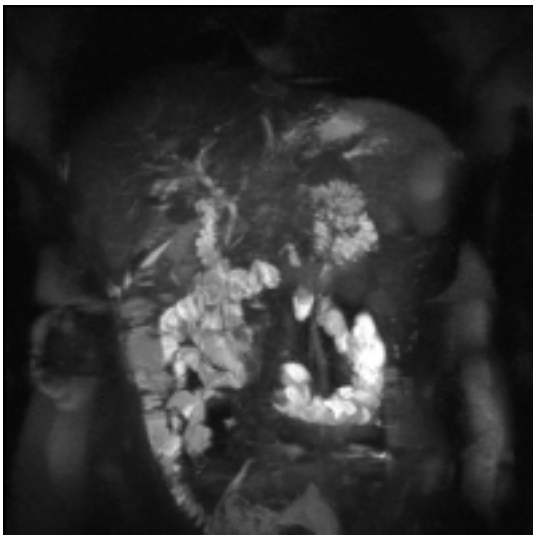

(a)

(b)

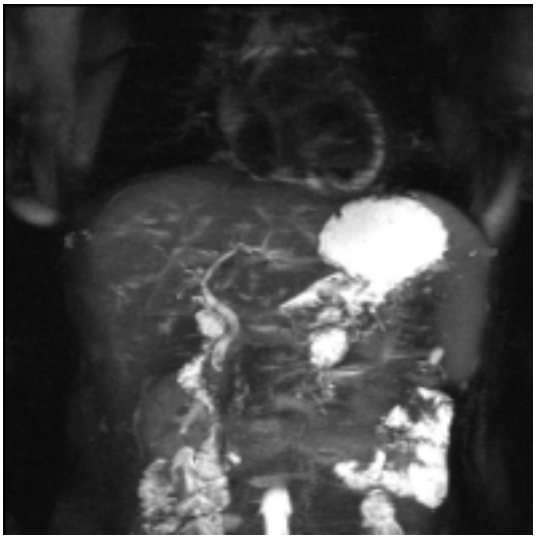

(c)

(d)

Figure 6. Results obtained on various data sets (continued).

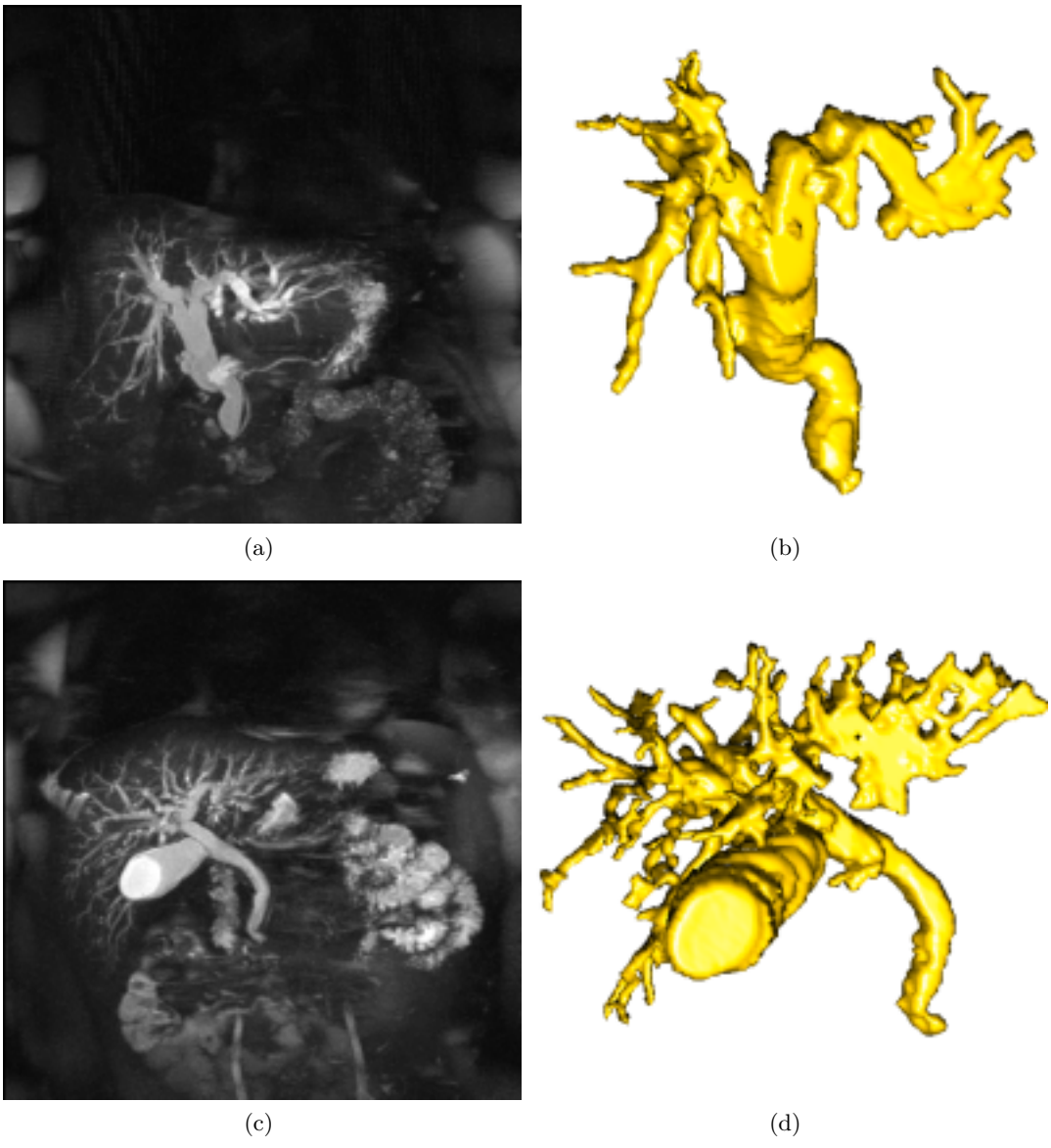

(a) (b)

(c) (d)

Figure 7. Results obtained on various data sets (continued).

- *Resolution compensation*: accounting for partial volume effects may allow for improved handling of the limited resolution available, facilitating the generation of high quality two and three dimensional data review from any angle.

With this programme of research a set of assistive image analysis tools and techniques is being developed which will lead to the production of an MRCP review station capable of providing the radiologist with a superior methodology for handling the review and assessment of MRCP examinations.

REFERENCES

1. J. Sai and J. Ariyama, *MRCP: Early Diagnosis of Pancreatobiliary Diseases*, Springer-Verlag, 2000.
2. J. Larena, E. Astigarraga, I. Saralegui, A. Merino, A. Capelastegui, and M. Calvo, "Magnetic resonance cholangiopancreatography in the evaluation of pancreatic duct pathology," *British Journal of Radiology* **71**, pp. 1100–1104, 1998.
3. D. Williams, K. Vitellas, and D. Sheafor, "Biliary cystadenocarcinoma: Seven year follow-up and the role of mri and mrcp," *Magnetic Resonance Imaging* **19**, pp. 1203–1208, 2001.
4. Y. Tang, Y. Yamashita, Y. Abe, T. Namimoto, T. Tsuchigame, and M. Takahashi, "Congenital anomalies of the pancreaticobiliary tract: Findings on mr cholangiopancreatiography (mrcp) using half-fourier-acquisition single-shot turbo spin-echo sequence (haste)," *Computerized Medical Imaging and Graphics* **25**, pp. 423–431, 2001.
5. X. Lin, Y. Sun, J. Hu, C. Ko, C. Chen, and T. Wang, "Three-dimensional reconstruction of the biliary tract from two-dimensional biliary images," *Endoscopy* **27**, pp. 400–403, 1995.
6. C. Ko, Y. Sun, C. Mao, and X. Lin, "Three-dimensional reconstruction of biliary tract from biplane projections," *Computer Methods and Programs in Biomedicine* **47**, pp. 21–33, 1995.
7. E. Neri, P. Boraschi, G. Braccini, D. Caramella, G. Perri, and C. Bartolozzi, "Mr virtual endoscopy of the pancreaticobiliary tract," *Magnetic Resonance Imaging* **17**(1), pp. 59–67, 1999.
8. P. Felkel, "Segmentation of vessels in peripheral cta datasets: Literature review and first tests of some approaches," tech. rep., VRVis Research Center for Virtual Reality and Visualization, 2000.
9. A. Frangi, W. Niessen, R. Hoogeveen, T. vanWalsum, and M. Viergever, "Model-based quantitation of 3-d magnetic resonance angiographic images," *IEEE Transactions on Medical Imaging* **18**(10), pp. 946–956, 1999.
10. A. Taleb-Ahmed, X. Leclerc, and T. SaintMichel, "Semi-automated segmentation of vessels by mathematical morphology : Application in mri," in *Proc. International Conference on Image Processing*, S. Cantu, ed., pp. 1063–1066, (Aristotle University of Thessaloniki, Greece), 2001.
11. J. Serra, *Image Analysis and Mathematical Morphology*, Academic Press, 1982.
12. P. Soille, "Mathematical morphology for image analysis and pattern recognition," tech. rep., Ecole des Mines d'Alès, 1998.
13. L. Vincent and P. Soille, "Watersheds in digital space: An efficient algorithm based on immersion simulations," *IEEE Transactions on Pattern Analysis and Machine Intelligence* **13**(6), pp. 583–598, 1991.
14. W. Lorensen and H. Cline, "Marching cubes: A high resolution 3d surface construction algorithm," *Computer Graphics* **21**(4), pp. 163–169, 1987.
15. J. Foley, A. van Dam, S. Feiner, J. Hughes, and R. Phillips, *Introduction to Computer Graphics*, Addison-Wesley, 1993.